W. M. KECK OBSERVATORY
Instrument Program Management

NGAO Science Instrumentation

Design Concept
September 14, 2009
By Sean Adkins

INTRODUCTION

Based on the science requirements for the Next Generation Adaptive Optics (NGAO) system under development by the W. M. Keck Observatory (WMKO) as given in the NGAO Science Case Requirements Document or SCRD ("Keck," 2008) we are proposing to develop an instrumentation capability for NGAO that provides imaging and integral field spectroscopy over the wavelength range of 0.818 to 2.4 μm. The NGAO project is operating in a challenging design and build to cost environment, with a strict upper bound on the overall cost including the initial science instrumentation.

Based on the science driven requirements described in the SCRD a set of baseline capabilities (Adkins et al., 2009) were developed that reflected both the needs of the science cases and the anticipated technical performance of the NGAO system (Dekany et al., 2009). These baseline capabilities have been combined with a well informed understanding of the most significant cost drivers to develop a concept for a single science instrument offering both imaging and integral field spectroscopy that fits within the NGAO cost limitations. This document describes the concept for this instrument and gives first order designs for the optical, mechanical, electronic, and software components of the instrument. These descriptions are followed by a brief description of the initial project plan for the design activities.

BASELINE CAPABILITIES

The proposed baseline capabilities for the NGAO science instrument are summarized in Table 1. The values of relevant parameters are given for the two desired modes, integral field spectroscopy, and imaging. The parameters are listed this way for clarity, but both capabilities will be provided in a single instrument.

While the current baseline capabilities cover the wavelength range of 0.818 to 2.4 μm the possibility exists that the short wavelength cut-off could be extended to provide access to Hα (656.3 nm). With the right coating choices the AO system for NGAO should be able to provide good throughput at these shorter wavelengths, but the optical design of the science instrumentation may become more challenging.

The imaging capability is expected to support diffraction limited imaging with high throughput and appropriate background suppression in order to take advantage of the low backgrounds provided by NGAO. The imaging capability must also provide a coronagraph to support the detection and characterization of planets around nearby low mass stars. The imager pixel scale will be λ/2D or smaller at the short wavelength cut-on of each wavelength band. Several pixel scales may be provided, additional study and simulation is required to establish the exact number of pixel scales required.

The integral field spectrograph (IFS) capability is expected to offer a spatial sampling scale optimized for the ensquared energy of the NGAO system in the near IR bands, and at least λ/2D at the short wavelength cut-on of the near-IR Y band. The initial approach to managing the field of view (FOV), spatial and spectral sampling, and spectral coverage trade offs inherent in an IFS design is to emphasize performance with narrow band (~5% band pass) filters. Larger band passes are not excluded, but a reduction in FOV will result, and depending on the imaging slicing approach implemented in the IFS broad band operation may add some complexity to the design.

Capability	Integral Field Spectrograph	Imager
Wavelength Coverage	z, Y, J, H, K (0.818 to 2.4 μm)	z, Y, J, H, K (0.818 to 2.4 μm)
Filters	Narrowband in z, Y, J, H, K, nominally 5% band pass per filter, number of filters as required to each band	See Table 2.
Spectral Resolution	~4000	1
FOV	~ 4" x 4" with 50 mas sampling	≥ 15"
Spatial Sampling	3 scales maximum: • 10 mas • 50 to 75 mas, spatial sampling selected to match 50% ensquared energy delivered by NGAO narrow field relay • Intermediate scale, possibly 20 or 35 mas, selected to balance FOV/sensitivity trade off	≤ λ/2D, possibility of multiple pixel scales
Coronagraph		6λ/D occulting spot, apodized pupil
Throughput (instrument only)	~40%	> 60% (without coronagraph)
Detector	4096 x 4096 (Hawaii-4RG)	4096 x 4096 (Hawaii-4RG)
Detector Performance	Background limited	Background limited or detector limited depending on observing band

Table 1: NGAO science instrument capabilities

Imaging applications are understood to require a selection of filters that include both the standard photometric band passes, and a selection of specialized filters matched to various diagnostic lines. This filter set will require additional study, but as a starting point a filter set based on the filters provided by the NIRC2 instrument is listed in Table 2.

Filter #	Filter Name	Cut-on λ (μm)	Cut-off λ (μm)	Notes
1	NGAO Y	0.970	1.07	UKIDSS photometric
2	NGAO J	1.170	1.330	UKIDSS/Mauna Kea photometric
3	NGAO H	1.490	1.780	UKIDSS/Mauna Kea photometric
4	NGAO K	2.030	2.370	UKIDSS/Mauna Kea photometric
5	Ks	1.991	2.302	Similar to NIRC2
6	Kp	1.948	2.299	Similar to NIRC2
7	J continuum	1.2033	1.2231	Similar to NIRC2
8	H continuum	1.5688	1.592	Similar to NIRC2
9	K continuum	2.2558	2.2854	Similar to NIRC2
10	Bracket γ (1)	2.1523	2.1849	Similar to NIRC2
11	Bracket γ (2)	2.1426	2.178	Similar to NIRC2
12	CO	2.2757	2.3024	Similar to NIRC2
13	CH_4S	1.5295	1.6552	Similar to NIRC2
14	CH_4L	1.6125	1.7493	Similar to NIRC2
15	FeII	1.6327	1.6583	Similar to NIRC2
16	He 1 B	2.04	2.0726	Similar to NIRC2
17	H2, v = 1-04	2.04	2.0726	Similar to NIRC2
18	H2, v = 1-04	2.2428	2.2816	Similar to NIRC2
19	Pa β	1.2807	1.3	Similar to NIRC2

Table 2: Imager filter set

INSTRUMENT CONCEPT OVERVIEW

The approach to science instrumentation for NGAO is based on a design and build to cost approach supported by six principles:

1. Ensure that the instrument capabilities are well matched to key science requirements
2. Ensure that the instrument capabilities are matched to the to AO system in order to maximize the science gains
3. Understand which requirements drive cost
4. Resist the temptation to add features
5. Maximize heritage from previous instruments
6. Evaluate ways to break the normal visible/near-IR paradigm of using different detectors in separate instruments

The concept developed for the NGAO science instrument is aimed at satisfying principles 1 and 2 as fully as possible. The main aspects of the concept as described here are then intended to address the remaining principles with a clearly cost driven approach supported by sound engineering and technical decisions. The design adopts specific subsystem design approaches, and some significant portion of subsystem designs from previous instruments, in particular the MOSFIRE (McLean et al., 2008) and OSIRIS (Larkin et al., 2006) instruments. A particular aspect of this design concept is to incorporate two instrument capabilities (imaging and spectroscopy) in a single cryogenic dewar with common fore-optics. The single dewar eliminates a significant cost component by eliminating the need to duplicate the dewar and a number of control systems such as temperature control and supervisory systems such as pressure monitoring.

A second important aspect of the design concept addresses principal 6, and that is the use of substrate removed HgCdTe infrared focal plane arrays (FPAs). The substrate removed FPAs have good (~70%) QE down to 500 nm, and although the single CDS read noise is higher than typical science grade CCDs (~15 e^-/read for a Hawaii-2RG vs. 5 e^-/read for a deep depletion CCD, see Adkins, 2009b) the low power dissipation of the FPA read out integrated circuit and non-destructive pixel read out allows many Fowler or up the ramp samples and results in essentially the same readout noise levels for exposures when the exposure duration allows time for the required number of reads. The result is that while the QE of CCDs will be at least 20% higher at 1 μm and below, this seems to be the only penalty for not using a CCD for the NGAO instrument below 1 μm. This represents another important component of the cost reduction needed in order to ensure the instrument supports the NGAO design/build to cost requirement.

A block diagram of the NGAO science instrument is shown in Figure 1. The instrument is a fully cryogenic infrared and optical (to ~0.818 μm) imager and IFS enclosed in a vacuum dewar. The dewar contains two optical systems, one for the imager shown in the upper portion of the block diagram, and one for IFS, shown at the bottom center of the block diagram. The FOVs of the imager and IFS are both at the center of the NGAO science FOV as illustrated in Figure 2. Starting at the top left side of the block diagram, light enters the dewar from the AO system through a vacuum window ~ 90 mm in diameter. The window is coupled to the NGAO system's cooled enclosure via a light and air tight bellows. The bellows isolates the two structures mechanically, and since the AO enclosure is cooled to about -18 °C (the exact temperature is to be confirmed) and filled with dry air, the emissivity of the window is reduced and the issue of condensation or ice on the window is eliminated during normal operation. A mechanism such as a dry air purge will need to be provided for the window during servicing or testing to prevent condensation when the window is exposed to ambient conditions.

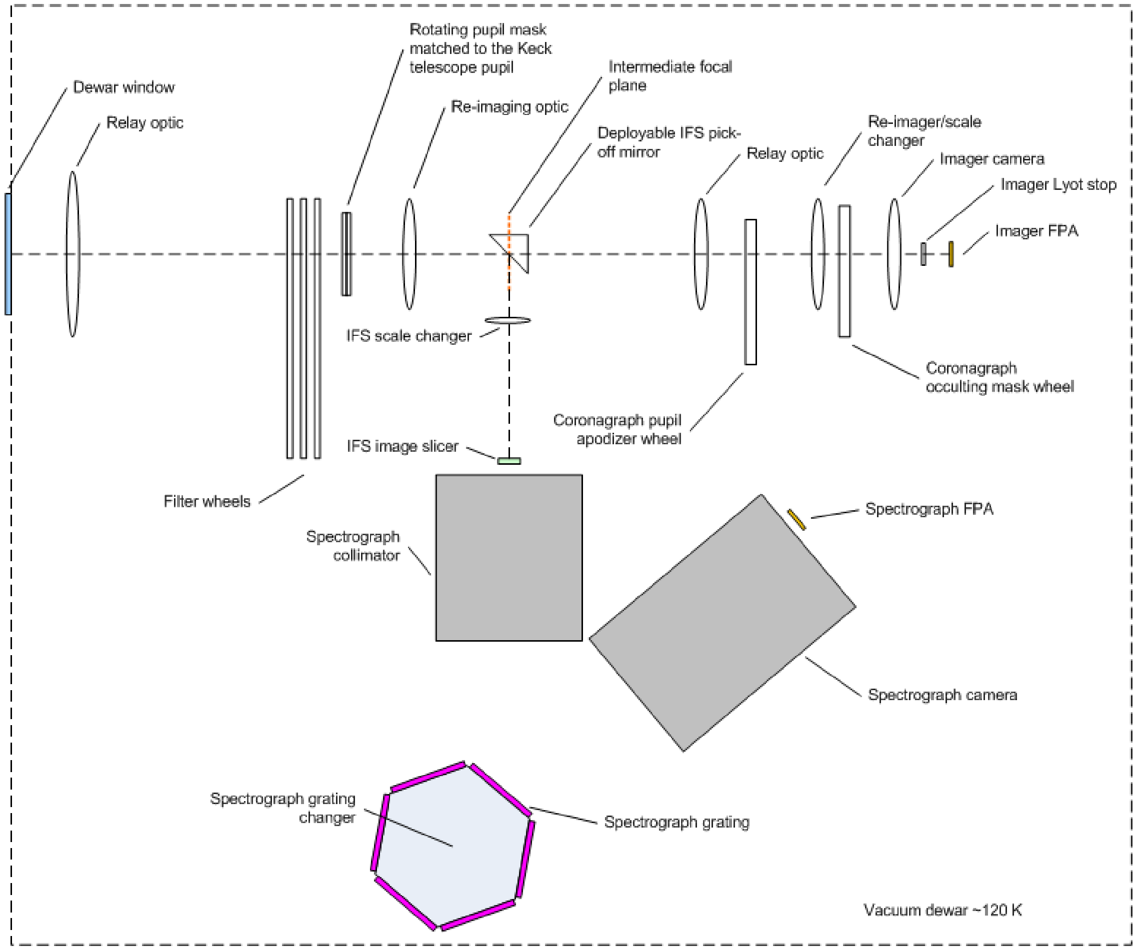

Figure 1: NGAO science instrument opto-mechanical block diagram (not to scale)

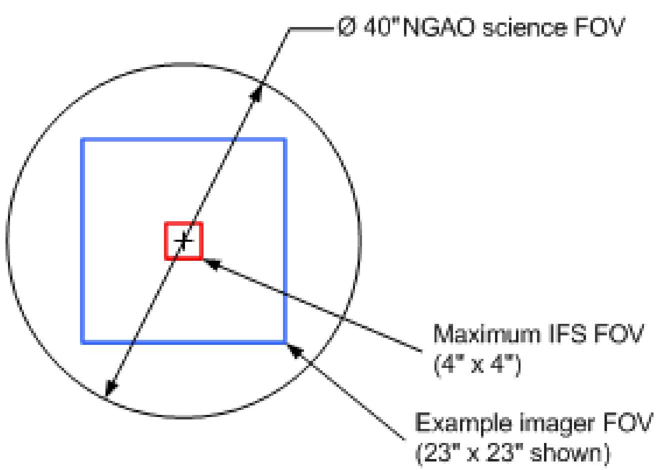

Figure 2: NGAO science instrument FOVs

The AO system's science focal plane is located inside the dewar at a relay optic that forms a pupil image on a tracking pupil mask matched to the primary mirror aperture and central obscuration of the Keck telescope. A set of filter wheels is located just in front of the pupil plane, with ~34 filters shared between the imager (19) and the IFS (15). Each wheel will contain ~9 filters plus an open position. After the pupil mask a re-imaging optic forms an intermediate focal plane at a reduced plate scale. Continuing to the right along the imager optical path this intermediate focal plane is followed by a second relay optic that forms a pupil image at a wheel carrying a selection of a series of pupil apodization masks for an apodized pupil Lyot coronagraph (APLC). The beam is then re-imaged at a second intermediate focal plane at a wheel carrying a selection of coronagraph occulting masks. Each wheel will have at least 4 masks plus an open position. After the second intermediate focal plane the image is formed on the detector by a camera. The imager will have three plate scales, and the exact method of scale changing has not been finalized, it will either be accomplished by the re-imaging optics, or by using different cameras.

Returning to the center of the diagram, the optical path to the IFS starts with a deployable pick-off mirror located near the first intermediate focal plane. This mirror sends the center of the intermediate focal plane to the IFS shown at the bottom center of the block diagram. The beam enters the IFS scale changer, which has three selectable scale changing optics to provide three spatial sampling scales for the IFS. The scale changer focuses the light on the IFS image slicer (baselined as a 96 x 96 lenslet array) and is then collimated by a three mirror anastigmat (TMA). The collimator TMA illuminates a grating working in the first order, and the dispersed light is then imaged onto the spectrograph detector by a second TMA. Multiple gratings will be used with a rotary grating changer to select the appropriate grating for each waveband.

OPTICAL DESIGN CONCEPT

A first order optical layout developed in Zemax is shown in Figure 4. This layout is based on version 7[1] of the NGAO optical design for the AO system (Kupke, 2009). The layout employs paraxial lenses for powered optics and is intended to identify the functional elements of the instrument's optics, provide an estimate of the overall path length, and point out the challenging areas of the design.

AO System Characteristics

The AO system optical design provides a focus for the science instrument with the following characteristics:

- A nominal f/46 beam with an unvignetted 40" diameter FOV
- Telecentric output (image of the telescope primary at infinite conjugate) with a focal plane radius of curvature of 300 mm
- Diffraction limited on-axis performance at 1 µm (9 mas rms spot radius)
- An NGS mode that introduces a transmitting dichroic (to the science instrument) tilted at 25º with respect to the science instrument's optical axis
- Predicted transmission of 45 to 60% over the NGAO passbands from 0.818 to 2.4 µm (Figure 3)

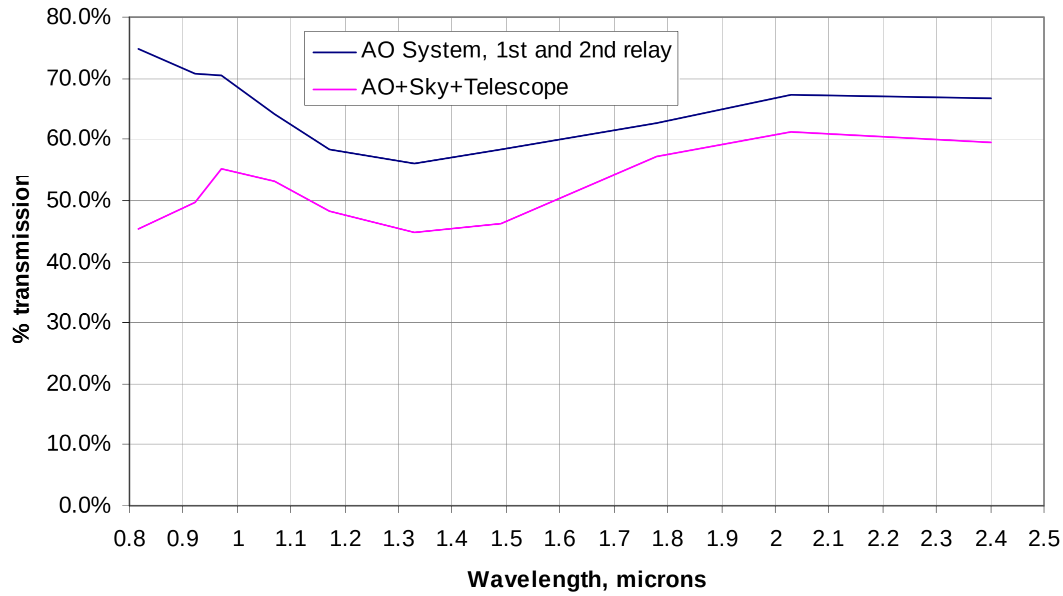

Figure 3: Predicted AO system transmission

[1] KNGAO_1-tier_100mm_120arcsec_straightthru_2nd-relay_wtelescope_v7.ZMX

The predicted transmission for the AO system shown in Figure 3 is based on the NGAO transmission budget flowdown spreadsheet[2] and includes all of the AO system surfaces in the science instrument optical path. The NGAO passband definitions are found in KAON-554 (Adkins, 2009a).

The f/46 beam was chosen to allow for sufficient path length from the AO system to include the NGS dichroic, and the possibility of multiple science instrument feeds in the future. As we will discuss, this also has an important influence on the path length of the instrument's internal optics.

First Order Optical Layout

The instrument's optics are fully cryogenic, with the AO system focal plane located inside the dewar, approximately 75 mm behind the dewar entrance window. A first order optical layout for the imager optics is shown in Figure 4. Starting in the upper left corner of Figure 4 relay E1 is located at the AO system's output focal plane and forms an image of the pupil on a mask matched to the telescope primary mirror and having a circular mask in the center for the secondary obscuration. The focal length of E1 was chosen to help reduce the path length and still produce what seems to be a tractable size for a pupil mask fabricated either by photo-etching or wire EDM, but it is probably too small to permit re-use of the MOSFIRE rotatable hexagonal mask that converts to a circular, slightly undersize pupil. Another option may be to consider basing the design on the NIRC2 pupil mask mechanism.

The mask provided with a rotator to compensate for the rotation of the telescope pupil introduced by the AO system's K-mirror image de-rotator. As shown in Figure 1 a set of filter wheels is located prior to the pupil mask. After the pupil mask, re-imager E2 forms an intermediate focal plane and in conjunction with relay E1 changes the focal ratio from f/46 to f/10.6. The choice of f/10.6 is somewhat arbitrary, but reflects the apparent necessity to reduce the path lengths inside the instrument.

At the intermediate focal plane a deployable pick-off mirror (~6" diameter, not shown in Figure 4) is used to send a square FOV of about 4" x 4" at the center of the science field to the IFS channel of the instrument. The intermediate focal plane is located ~184 mm from relay E2. Relay E3 forms a pupil image on a selectable apodizing mask. Re-imager E4 creates a second intermediate focus for a coronagraph occulting mask and is followed by the camera for the imager. The Lyot stop for the coronagraph is located at a pupil plane prior to the imager's 4k x 4k Hawaii-4RG focal plane array. The camera in this layout also serves to match the scale of the intermediate focal plane to the detector. As can be seen from Figure 4 the AO system's focal plane curvature is simply applied to the detector, the field will have to be properly flattened in the final design. The camera in the first order optical layout results in an 8 mas pixel scale at the detector.

[2] NGAO_PD_Phase_Flowdown_Budgets_2003_Format.xls

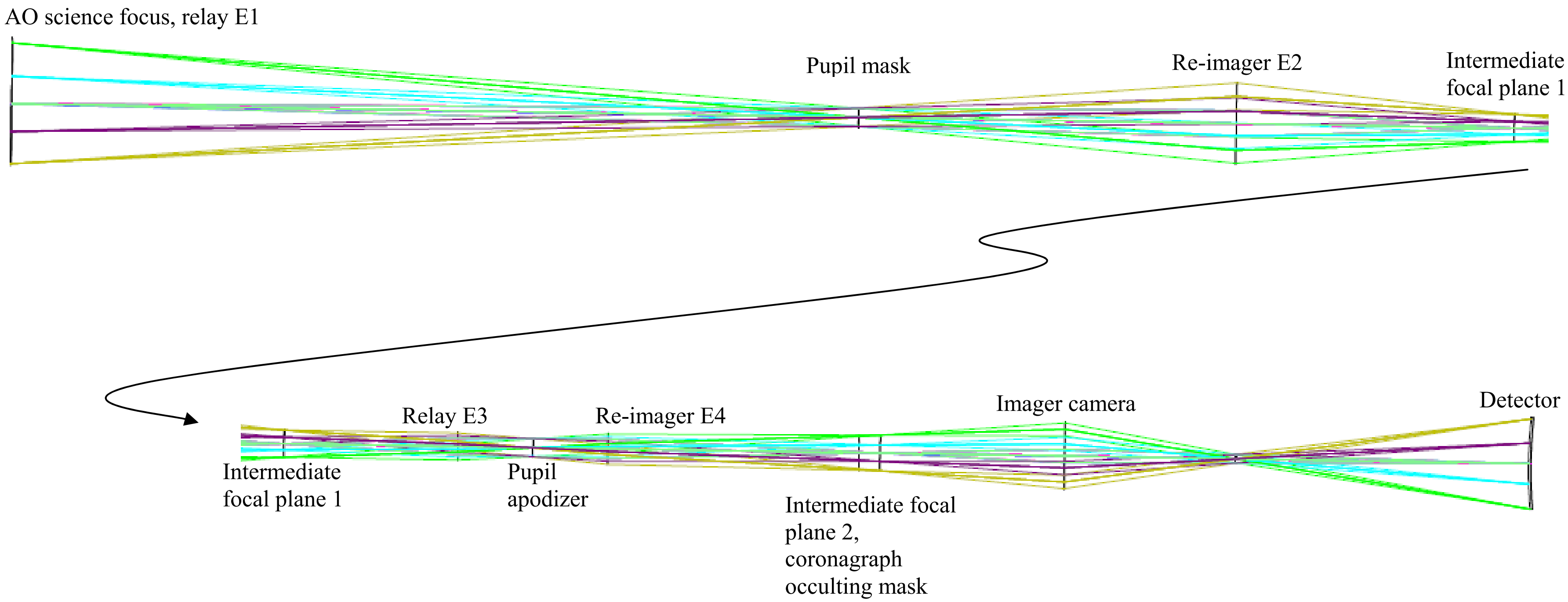

Figure 4: First order (paraxial) optical layout

Imager Plate Scales

While the imager would be simpler if a single plate scale were possible, it appears that sampling at 2 or 3 times the diffraction limit in each wavelength range is desirable to maximize the accuracy of representation for the flux distribution of point sources (see for example Baek and Marchis, 2007) and consequently maximize the accuracy of image position measurements, one of the contributions to astrometric accuracy. The 2 and 3 times sampling scales in mas at the short wavelength cut-on in each of the NGAO passbands are shown in Table 3.

	Wavelength, nm	λ/D(")	λ/2D(mas)	λ/3D(mas)
K band cut-on	2030	0.042	20.9	14.0
J band cut-on	1170	0.024	12.1	8.0
Y band cut-on	970	0.020	10.0	6.7
z band cut-on	818	0.017	8.4	5.6
i band cut-on	728	0.015	7.5	5.0
r band cut-on	565	0.012	5.8	3.9

Table 3: Imager sampling scales

The green highlighting in the table indicates what Baek and Marchis have identified as the preferred wavelength ranges for 2 and 3 times sampling. Based on this it appears that no more than three plate scales are required for the imager: 6, 8, and 14 mas. It may also be possible to have two (7 and 14 mas) or even one (7 or 8 mas), although the latter will result in significant over sampling in the K band. Depending on the complexity of the camera design this may be achieved by three different cameras, or by a single camera in conjunction with three sets of scale changing optics.

Optical Design Requirements

The design/build to cost approach for the NGAO science instrument creates a necessity for being creative with regards to design re-use, and careful with optical complexity. As discussed in the section on the mechanical design concept, it is thought that the MOSFIRE dewar design can be substantially reused for the NGAO instrument. While it might initially seem a bad idea to take a fairly long optical path and package it on a round optical table, the MOSFIRE dewar design represents a known cost with demonstrated thermal performance and this approach has advantages in terms of overall size, accessibility of components during assembly, alignment, and service. The MOSFIRE dewar design also employs shapes that minimize deflection of the dewar walls, and is a shape that has been used to package a number of other infrared instruments (Bonnet, 2004; Ulrich Käufl, 2008).

Taking the optical layout of Figure 4 and folding into a footprint compatible with a round optical table will require introducing one or more fold mirrors, or employing the powered optical surfaces as fold optics by using reflective elements. It is not clear at this point whether a refractive or reflective design is more desirable. Given the wavelength range that the instrument is expected to cover (from 0.818 to 2.4 μm, with a possibility of shortening the cut-on wavelength) some optical performance requirements may be easier to meet with a reflective design. On the other hand the image quality requirements may be easier to meet for a given cost with a refractive optical system.

The trade-off between reflective or refractive needs to be considered early in the design and a combined refractive/reflective design is a possibility. Note that this discussion applies to the instrument's fore-optics and imager optics, it is anticipated that a three mirror anastigmat design will be used for the IFS collimator and camera.

The next step in the development of the optical design is to replace the layout using paraxial elements with a design using real optical elements. To guide that activity Table 4 gives the goals for the optical performance of the imager. These requirements are derived from the baseline capabilities summarized in Table 1 and the 30 nm rms of uncorrectable (non-common path) wavefront error allocated to the science instrument in the NGAO flowdown budget.

Table 4: NGAO instrument optical performance goals

Parameter	*Goal*	*Min.*	*Max.*	*Units*	*Notes*
Image quality					
Imager	< 0.5	-	1	µm	1
IFS	> 80	70	-	% ensquared energy	2
Wavefront error					
On-axis	<30	-	30	nm, rms	3
Off-axis	<60	-	60	nm, rms	4
Distortion					
Imager	< 0.25	-	0.5	%, peak to peak	5
Optical throughput					
Imager					
NGAO z'	> 70	60	-	% at 0.87 µm	6
NGAO Y	> 70	60	-	% at 1.00 µm	6
NGAO J	> 70	60	-	% at 1.25 µm	6
NGAO H	> 70	60	-	% at 1.64 µm	6
NGAO K	> 60	55	-	% at 2.2 µm	6
IFS					
NGAO z'	≥ 50	40	-	% at 0.87 µm	7
Y-band	≥ 50	40	-	% at 1.00 µm	7
J-band	≥ 50	40	-	% at 1.25 µm	7
H-band	≥ 50	40	-	% at 1.6 µm	7
K-band	> 40	40	-	% at 2.2 µm	7
Non-uniformity					
Imager	< 5	-	10	%, peak	8
IFS	< 5	-	10	%, peak	8
Instrument background					
Y-band	< 0.001	-	0.02	e^-/sec/pixel	9
J-band	< 0.001	-	0.02	e^-/sec/pixel	9
H-band	< 0.001	-	0.02	e^-/sec/pixel	9
K-band	< 0.001	-	0.02	e^-/sec/pixel	9
Ghosting					
Imager	$< 10^{-5}$	-	$< 10^{-4}$	-	10
IFU	$< 10^{-5}$	-	$< 10^{-4}$	-	10

Notes:

1. Area weighted average rms diameter over the wavelength range of 0.818 to 2.40 μm.
2. Ensquared energy in a 2 x 2 pixel box centered on the image centroid over the wavelength range of 0.818 to 2.40 μm.
3. Total on-axis rms wavefront error for the imager, total rms wavefront error for the IFS optical path to the image slicer (lenslet array).
4. Total rms wavefront error at 20" radius for the imager, total rms wavefront error at 20" radius for the IFS optical path to the image slicer (lenslet array).
5. Total geometric distortion over the entire imager FOV. The intent is to limit the instrumental contribution to astrometric error to < 0.05 mas rms for the 8 mas plate scale.
6. Imager throughput, without coronagraph, QE of the science detector is not included.
7. IFS throughput, QE of the science detector is not included.
8. This is the peak variation in transmission over the full FOV.
9. This is the contribution of the instrument background to the total "dark counts"; the goal value is 10% of the goal for science detector dark current.
10. Intensity of the ghost image compared to the parent image at all wavelengths from 0.818 to 2.40 μm.

Pupil Mask

A rotating pupil mask, matched to the shape of the Keck telescope primary, and provided with a mask for the telescope's center obscuration is essential to achieving low backgrounds, especially in the K band. The quality of the pupil image formed on the mask will be important and it will also be important to understand, and if possible control the amount of wavelength dependent pupil motion and diffraction in order to ensure that the background control needs are satisfied without undue loss of light or vignetting. If necessary more than one pupil mask can be provided, but a pupil mask matched to the shape of the telescope aperture will need to rotate to compensate for the rotation of the telescope aperture by the AO system's image de-rotator will make interchangeable masks more complex. In the current optical layout the pupil image may be too small to accommodate a variable tracking/circular mask as used in the MOSFIRE instrument (the MOSFIRE pupil is 125 mm in diameter), but it may be appropriate to consider a larger pupil image so that a similar design can be used. Note that the pupil mask only needs to rotate when it is of a shape matched to the shape of the telescope primary aperture.

Coronagraph Requirements

The starting point for the imager's coronagraph is the NGAO system design phase discussion of coronagraph performance for the imaging and characterization of extrasolar planets around nearby stars found in Flicker et al. (2007). An apodized pupil Lyot coronagraph (APLC) with an occulting spot of 6λ/D, 10λ/D, and 14λ/D was analyzed using a numerical simulation for a 30 minute J band exposure. The analysis concludes with the observation that while not all of the science cases can be satisfied by this configuration it is capable of addressing a useful fraction (~50%) of the extrasolar planet observing scenarios. As a starting point we assume a 6λ/D coronagraph for the NGAO imaging capability, but further simulation work using the current predictions for NGAO performance are required.

The NGAO instrument's APLC consists of a hard edged coronagraph mask located at the first intermediate focal plane after relay E2, an apodizing plate located at a pupil image formed by relay E3, and a Lyot stop at the pupil of the imager's camera.

For each of the NGAO passbands (Adkins, 2009a) the required scales for the coronagraph occulting spots at 6λ/D are given in Table 5. The table also indicates the Airy ring size (λ/D, where D = 10 m), and the physical size of a sharp edged occulting spot taking into account the plate scale at the intermediate focal plane of 0.565 mm/". The full aperture at the intermediate focal plane is 18.5 mm diameter in the first order optical layout. Note that it may not be necessary to include all of the occulting spot sizes listed in Table 5, in particular a larger spot may be better the at shorter wavelengths due to the decreasing Strehl ratio.

Soummer et al. (2009) discuss the application of a prolate spheroidal function to the design of the apodizer, and they suggest that a circular mask provides slightly better performance than a hexagonal mask in the case of a telescope with a hexagonal pupil such as the Keck telescopes. Soummer also discuss the sizing of the Lyot stop and indicate that with an APLC the Lyot stop does not have to be undersized as it would be in a simple Lyot coronagraph. However, assuming a circular aperture the Lyot stop will have to be sized to inscribe the circular aperture on the primary mirror footprint, resulting in an outer obscuration of ~8 %.

	Wavelength, nm	λ/D (Airy disk dia. in mas)	6λ/D corongraph spot size (mas)	Coronagraph spot dia. (mm)
K band cut-on	2030	41.9	251.2	0.445
J band cut-on	1170	24.1	144.8	0.256
Y band cut-on	970	20.0	120.0	0.213
z band cut-on	818	16.9	101.2	0.179
i band cut-on	728	15.0	90.1	0.160
r band cut-on	565	11.7	69.9	0.124

Table 5: Coronagraph occulting spot sizes

There are other possibilities for the configuration of the coronagraph that will be explored during the development of the optical design. One of these that may reduce the complexity, at least slightly, is to place the pupil apodizing mask at the pupil of the second AO relay. This would eliminate a cryogenic mechanism for pupil mask deployment. The relay element E1 in the NGAO instrument's optical path can be moved past the AO focal plane with minimal impact, and the coronagraph occulting spot can be placed at the AO focus inside the dewar. The pupil mask after relay E1 will then serve as the Lyot stop for the coronagraph. This would eliminate relay E3 and re-imager E4, and the cold stop in the scale changer or imager camera. Another option if it is desirable to keep relay E3 and E4 might be to use the IFS pick-off translation stage to also carry the coronagraph mask or masks (requiring a longer axis of motion of course).

Scale Changers and Camera

The first order optical layout requires a camera operating at f/2 for the 8 mas scale of the imager. To realize the other two plate scales (6 mas and 14 mas) a scale changing configuration or three separate cameras could be used. The first order optical layout implies an f/2.6 camera for the 6 mas plate scale, and an f/1.1 camera for the 14 mas plate scale. It would be desirable to adjust the focal reduction prior to the camera to increase these f-numbers.

IFS

The overall arrangement proposed for the IFS is shown in the lower center of Figure 1. A pick-off mirror located near the intermediate focus sends the central portion of the beam, corresponding to the maximum FOV of the IFS (4" x 4") to the IFS optical system. It may be useful to allow the imager to minimize the vignetting of the imager field by the IFS pick-off, and to control scattering due to the pick-off mechanism. If this is done then simultaneous imaging and IFS observations may be possible. Note also that a variation on the pick-off design could be considered by using a partially silvered pick-off mirror, allowing the central object to be used for PSF imaging at the same time as an IFS observation. The added complexity of more than one pick-off mirror must be carefully evaluated.

After the pick-off mirror the f/10.6 intermediate focus is changed in scale to produce the desired sampling scales on the lenslet array. For a 200 μm lenslet array pitch the scale changer f-numbers are shown in Table 6.

Spatial sampling scale	Scale changer f-number
10	377
35	108
50	75

Table 6: IFS scale changer f-numbers

The baseline configuration for the IFS employs a lenslet based image slicer similar to the OSIRIS instrument. The initial analysis presented in the following paragraphs was developed with reference to OSIRIS optical design notes (OODN0300 and OODN0400 by James Larkin). The lenslet array is located at the focus of the scale changer and forms a pupil image from each spatial sample that in turn becomes the effective entrance slit of the spectrograph. The lenslet array is rotated with respect to the spectrograph causing successive lenslets column wise to produce adjacent, staggered spectra on the detector. By choosing a rotation such that 24 such spectra are produced for each row wise step across the lenslet array, the 4096 pixel wide Hawaii-4RG detector will accommodate 85 row wise steps. In the other dimension a total of 4 rows of staggered spectra can be accommodated with ~1024 pixels per spectrum for a total of 85 x 96 spectra on the detector. The 1024 pixels per spectrum imply that narrow band filters are used to limit the length of each spectrum.

Using an 85 x 85 lenslet array with a pitch of 200 μm results in a total area of 17 mm x 17 mm for the lenslet array (compared to the OSIRIS lenslet array of 16 mm x 16 mm). The lenslet array is rotated with respect to the spectrograph to produce 24 staggered spectra corresponding to 24 columns of lenslets (compared to 16 in OSIRIS). With a 50 mas spatial scale the 85 x 85 lenslet array will result in an FOV of 4.25".

The pupil size at the spectrograph based on 200 μm lenslets and 24 spatial samples (lenslet columns) in the space of one lenslet pitch (1/24 stagger) is 8.3 μm for the 50 mas plate scale. The f-number of the lenslets is 3.4, and the collimator should match this f-number. With a larger detector (Hawaii-4RG) the spectrograph camera will require a somewhat larger field size (~1.6 times on each axis), but the required f-number is only 11.35 based on a 17 mm x 17 mm lenslet array and 15 µm detector pixels.

The focal length of the collimator will be determined by requirements to illuminate the proper area on the grating, and the combined focal length of the collimator and camera will be selected to ensure that the spectra are properly imaged on the detector. The baseline concept is to use a different grating for each of the instrument's passbands as shown in Table 7. For efficiency the gratings will be chosen to operate close to the blaze condition ($\alpha - \theta_B = \beta - \theta_B$).

	Wavelengths		
Passband	**cut-on (µm)**	**cut-off (µm)**	**center (µm)**
NGAO z spec	0.855	1.05	0.9525
NGAO Y spec	0.97	1.12	1.045
NGAO J spec	1.1	1.4	1.25
NGAO H spec	1.475	1.825	1.65
NGAO K spec	2	2.4	2.2

Table 7: IFS passbands

Stock gratings would be desirable from a cost standpoint, and Table 8 lists some possible candidates from the Newport Richardson stock list of plane ruled reflectance gratings.

Passbands	**Catalog Number**	**Grooves/ mm**	**Nominal Wavelength (1st order, Littrow)**	**Blaze Angle**	**Ruled Area**
K	53-*-770R	300	2.0 µm	17.5°	154 x 206
H, J	53-*-590R	400	1200 nm	13.9°	154 x 206
Y, z	53-*-520R	600	1.0 µm	17.5°	154 x 206

Table 8: IFS grating candidates

MECHANICAL DESIGN CONCEPT

The key mechanical design feature of the NGAO science instrument is the re-use of the MOSFIRE dewar design. This may seem like an unusual choice but with appropriate modifications the concept has several benefits. First, the MOSFIRE dewar design represents a known cost with demonstrated thermal performance. Second, the dewar has a shape that minimizes deflection of the dewar walls, and is easily adapted for a fixed gravity orientation with the major axis of the dewar horizontal. Design details of the MOSFIRE dewar and internal structure may be found in the project's detailed design report ("MOSFIRE," 2007).

Dewar and Internal Structure

The MOSFIRE internal structure design is shown in Figure 5, taken from Figure 31 of the MOSFIRE detailed design report. The outer most portion of the structure is the composite support tube that provides a thermal stand-off for the instrument's internal structure. The front bulkhead (bulkhead A in the Figure) provides one of two main optical benches for mounting MOSFIRE's opto-mechanical systems. Bulkhead A is connected to a second bulkhead (bulkhead B) by a central tube and an outer support tube, these create a rigid structure that is essential to reduce flexure in MOSFIRE's variable gravity operating environment at the Keck I Cassegrain focus. Bulkhead B is the second main optical bench for MOSFIRE's opto-mechanics, and supports a continuation of the central support tube to a third smaller bulkhead where the MOSFIRE flexure control system (FCS) is mounted.

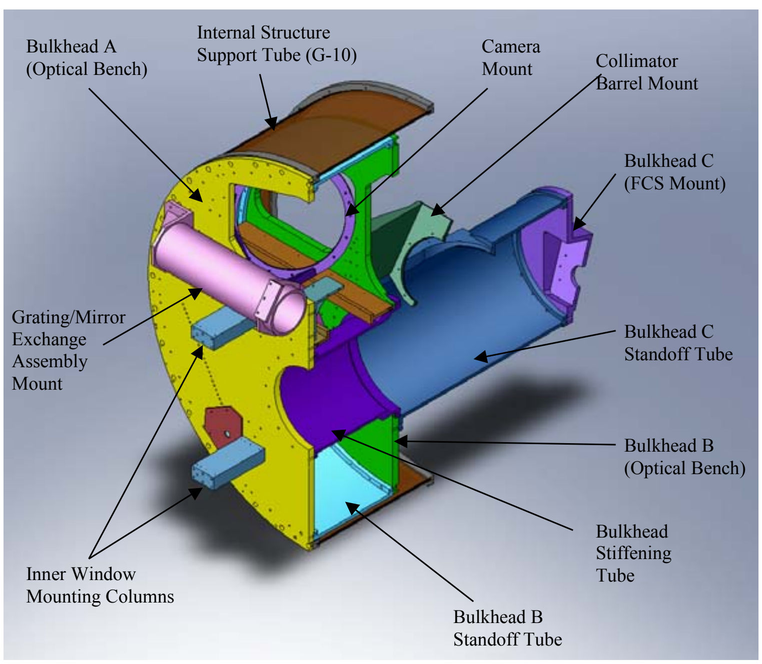

Figure 5: MOSFIRE internal structure (cross section)

The NGAO adaptation will eliminate the central support tube, the extension of the tube from bulkhead B, and bulkhead C. Most or all of bulkhead A will be eliminated, depending on the requirements for support of the IFS TMAs. The outer stand-off tube may need to be stiffened by additional structure to allow it to interface to the composite stand-off and support bulkhead B which will become the main optical bench for the instrument. The various other opto-mechanical support components shown in Figure 5 will be eliminated and the main optical bench layout will then be developed to match the requirements of the NGAO instrument's opto-mechanical systems.

There are some features of the MOSFIRE dewar design that are not needed. The NGAO instrument configuration will have the input light entering from a port on the side of the dewar rather than the front end cap, and the vacuum ports currently located on the front cap, which becomes the top cap, will be relocated to the rear cap. This will make the top cap a featureless dome shape. The rear cap will also be modified to eliminate the extension for the MOSFIRE FCS.

The baseline for the instrument's cryogenic cooling system will be to reuse the MOSFIRE design which employs two Brooks Automation (formerly CTI) model 1050 single stage closed cycle refrigerator (CCR) heads for cooling the dewar interior. The MOSFIRE detector is cooled by a model 350 two stage cold head, and two such cold heads will be required for the NGAO instrument. MOSFIRE is also equipped with a temperature stabilization system and uses variable speed drive for the cold heads. These features are also baselined for the NGAO instrument.

Mechanisms

The majority of the mechanisms required for the NGAO instrument can be implemented using straightforward rotary or wheel designs derived from the MOSFIRE and OSIRIS instruments. Referring to Figure 1 these include wheel mechanisms for the filters, coronagraph pupil apodizers, and coronagraph occulting masks. The instrument's two detectors may be equipped with focus mechanisms derived from MOSFIRE's detector head assembly as well. While the AO system will maintain the focus for the instrument, there are integration and test advantages to being able to shift the detector focus, and it may be important for observing efficiency to maintain parfocality between the imager and IFS channels.

The scale changer (or camera changer for the imager) mechanisms may also be implemented using a wheel design, but the instrument's wavefront error and pupil quality requirements may make these designs more demanding, and another design approach may have to be considered.

The three mechanisms that are unique to the NGAO instrument are the pupil mask rotator, the IFS pick-off mirror deployment mechanism, and the spectrograph grating changer. The design for the pupil mask rotator will depend on the size of the pupil mask that results from the preliminary optical design. At present it appears that the pupil mask will be relatively small. Another consideration is the possibility that various sizes of pupil mask may be needed for different wavelength bands. The simplest choice is likely to be a single mask, matched to the Keck telescope pupil and rotated by a microstepping drive using a cryogenic stepper motor.

The IFS pick-off mirror mechanism does not need to become too challenging, the tolerances on its motion can be relaxed by making the pick-off mirror oversize and by making the axis of deployment motion parallel to the angle for the mirror's surface that is needed to direct the input beam to the IFS. However, one advantage to having a mirror close to the required size for the 4" x 4" area of the focal plane is that vignetting of the imager will be reduced, allowing the possibility of simultaneous imaging and spectroscopy. Deployment of the IFS pickoff mirror can be accomplished with either a rotary mechanism or a linear slide mechanism. Cryogenic linear stages are available, and the load requirements will be modest. The exact angle of the fold introduced into the beam by the pick-off mirror will be determined by the preliminary optical design and opto-mechanical layout considerations, but this should not have a significant impact on selection of a mechanism for the pick-off mirror.

The third mechanism unique to the NGAO instrument is the grating changer. The proposed mechanism for this is a rotary turret carrying the gratings on an outer radius. Each grating can be mounted with precision adjustments to ensure proper alignment in the spectrograph. The requirements on positioning of the gratings will be demanding in order to ensure repeatability of instrument wavelength calibrations. It is likely that this motion axis will require high precision position encoding, perhaps by using either a series of LVDTs, or perhaps optical position sensing.

It should also be noted that all motors used in the mechanisms will require proper cold strapping and shielding to prevent thermal radiation into the optical path. It is expected that motors will be energized only during mechanism moves.

Interfaces

The mechanical interfaces between the NGAO instrument and the telescope/AO system will be simple, provided that analysis of the stability of the mounting of the instrument and the AO system to the Nasmyth platform will support the requirements for relative motion between the instrument and the AO system. This is understood to be primarily driven by the NGAO astrometry error budget.

The instrument will mount to the Keck II telescope left Nasmyth platform on kinematic mounting pads to allow adjustment of the instrument's position for alignment with the AO system's science focal plane. The dewar will be supported by a steel tube structure that mounts to the bottom of the dewar shell's main cylinder. This corresponds to the location where the MOSFIRE dewar is mounted to the Cassegrain rotator module using an offset steel web structure.

The interface to the AO system's bench enclosure that is used to insulate the cooled bench from the dome ambient will be accomplished by a bellows. This may require insulation or be of double wall construction to ensure the integrity of the AO system's interior.

ELECTRONICS

The NGAO instrument electronics will be derived directly from the MOSFIRE electronics design. An electronics rack cooled by a liquid to air heat exchanger will be mounted next to the dewar and will contain all of the electronics systems required by the instrument. A block diagram of the NGAO instrument electronics is shown in Figure 6.

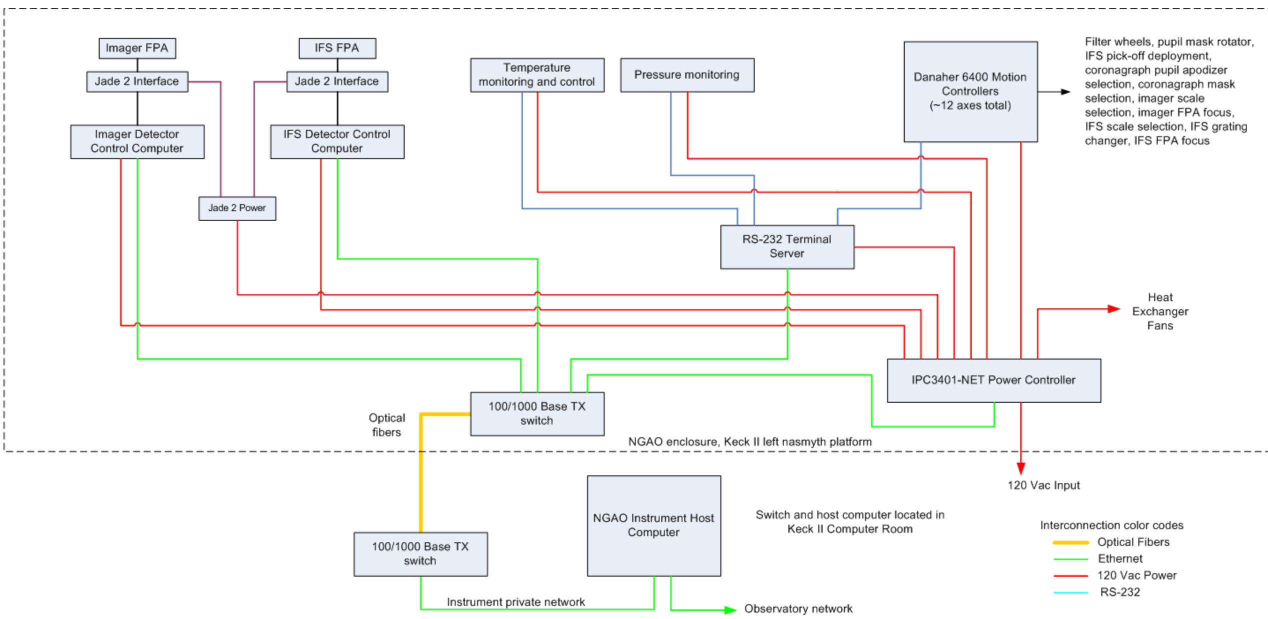

Figure 6: NGAO instrument electronics block diagram

SOFTWARE

The NGAO instrument software will be based on the software developed for the MOSFIRE instrument. The detector software, temperature and pressure monitoring, power controller and 6400 series motion controller software will be a straightforward port from MOSFIRE. The low level and global server architecture will also be re-used from MOSFIRE. The instrument graphical user interface (GUI) designs are TBD, but they could easily be based on a port of the MOSFIRE desktop and control GUIs.

REFERENCES

Adkins, S. (2009, January 9). Keck Next Generation Adaptive Optics System Passband Definitions. Keck Adaptive Optics Note 554. Waimea, HI: W. M. Keck Observatory.

Adkins, S. (2009, January 20). Keck Next Generation Adaptive Optics Detectors for NGAO Instrumentation. Keck Adaptive Optics Note 556. Waimea, HI: W. M. Keck Observatory.

Adkins, S., Larkin, J., Max, C. & McGrath, E. (2009, July 3). NGAO Science Instrumentation Baseline Capabilities Summary. Waimea, HI: W. M. Keck Observatory.

Baek, M. & Marchis, F. (2007, November 27). Next Generation Adaptive Optics: Optimum Pixel Sampling for Asteroid Companion Studies. Keck Adaptive Optics Note 529. Waimea, HI: W. M. Keck Observatory.

Bonnet, H., Conzelmann, R., Delabre, B., Donaldson, R., Fedrigo, E., Hubin, N. N., Kissler-Patig, M., Lizon, J., Paufique, J., Rossi, S., Stroebele, S. & Tordo, S. (2004). First light of SINFONI AO-module at VLT. *Proc. SPIE 5490*, 130-138.

Dekany, R., Neyman, C., Wizinowich, P., McGrath, E. & Max, C. (2009, March 10). Build-to-Cost Architecture Wavefront Error Performance. Keck Adaptive Optics Note 644. Waimea, HI: W. M. Keck Observatory.

Flicker, R., Macintosh, B., Dekany, R., Liu, M. & Neyman, C. (2007, June 27). NGAO High-Contrast & Companion Sensitivity Performance Budget (WBS 3.1.1.10). Keck Adaptive Optics Note 497. Waimea, HI: W. M. Keck Observatory.

Keck Next Generation Adaptive Optics Science Case Requirements Document. (2008, March 28). Keck Adaptive Optics Note 455 [Release 2.2]. Waimea, HI: W. M. Keck Observatory.

Kupke, R. (2009, June 11). Keck NGAO Relay Design.

Larkin, J.; Barczys, M.; Krabbe, A.; Adkins, S.; Aliado, T.; Amico, P.; Brims, G.; Campbell, R.; Canfield, J.; Gasaway, T.; Honey, A.; Iserlohe, C.; Johnson, C.; Kress, E.; LaFreniere, D.; Lyke, J.; Magnone, K.; Magnone, N.; McElwain, M.; Moon, J.; Quirrenbach, A.; Skulason, G.; Song, I.; Spencer, M; Weiss, J.; Wright, S. (2006). OSIRIS: a diffraction limited integral field spectrograph for Keck. New Astronomy Reviews 50(4-5), 362-364.

McLean, I. S., Steidel, C. C., Matthews, K., Epps, H. & Adkins, S. M. (2008). MOSFIRE: A multi-object near-infrared spectrograph for the Keck Observatory. *Proc. SPIE 7014*, 70142Z-70142Z-12.

MOSFIRE: Multi-Object Spectrograph for Infra-Red Exploration, detailed design report. (2007, April 6). http://irlab.astro.ucla.edu/mosfire/MOSFIRE%20DDR%20Report%20v2.pdf

Soummer, R., Pueyo, L., Ferrari, A., Aime, C., Sivaramakrishnan, A. & Yaitskova, N. (2009, April 10). Apodized pupil Lyot coronagraphs for arbitrary apertures. II: Theoretical properties and application to extremely large telescopes. *The Astrophysical Journal 695*(1), 695-706.

Ulrich Käufl, H. (2008). CRIRES: A High Resolution Infrared Spectrograph for ESO's VLT. In Precision Spectroscopy in Astrophysics, Proceedings of the ESO/Lisbon/Aveiro Conference [Aveiro, Portugal], 227-230.